DOI: 10.1021/ic1010665

Inorganic Chemistry
Article

Photoisomerizable Metallomesogens and Soft Crystals Based on Orthopalladated Complexes

M. J. Baena,[†] P. Espinet,*[,†] C. L. Folcia,[‡] J. Ortega,[§] and J. Etxebarría*[,‡]

[†]*IU CINQUIMA/Química Inorgánica, Facultad de Ciencias, Universidad de Valladolid, 47071 Valladolid, Spain,* [‡]*Departamento de Física de la Materia Condensada, Facultad de Ciencia y Tecnología, Universidad del País Vasco, Apartado 644, 48080 Bilbao, Spain, and* [§]*Departamento de Física Aplicada II, Facultad de Ciencia y Tecnología, Universidad del País Vasco, Apartado 644, 48080 Bilbao, Spain*

Received May 26, 2010

With the aim of obtaining light-responsive liquid-crystalline palladium complexes, six palladium complexes derived from an orthometalated imine, bearing one or two azocarboxylato bridges, have been synthesized: $[Pd_2(\mu\text{-}SC_{10}H_{21})(\mu\text{-}O_2CAzo)(L^{1,2})_2]$ (**7** and **8**), $[Pd_2(\mu\text{-}SC_{10}H_{21})(\mu\text{-}O_2CAzo3C_{10})(L^{1,2})_2]$ (**9** and **10**), $[Pd(\mu\text{-}O_2CAzo)L^1]_2$ (**11**), and $[Pd(\mu\text{-}O_2CAzo3C_{10})L^1]_2$ (**12**), in which L^1 = *p*-$H_{21}C_{10}OC_6H_3CH{=}NC_6H_4OC_{10}H_{21}$-*p*, L^2 = *p*-$H_{21}C_{10}OC_6H_3CH{=}NC_{14}H_{29}$, $AzoCO_2^-$ = *p*-(phenylazo)benzoate, and $Azo3C_{10}CO_2^-$ = *p*-(2′,3′,4′-tris-*n*-decyloxyphenylazo)benzoate. Three of them (**7**−**9**), as well as the precursor $Azo3C_{10}CO_2H$ (**3**), are thermotropic liquid crystals displaying nematic and smectic A mesophases, while **10**−**12** have been identified by X-ray diffraction to give rise to "soft" crystal phases. Electronic spectroscopy and ^1H NMR show that all of them undergo a trans−cis isomerization of the azobenzene moiety at λ = 365 nm. The molecular structure determines the photoresponse in solution, which is faster and more stable when the trisubstituted azocarboxylate is present and the motion of the azo group is not hindered by the orthometalated imine. The photoresponse has also been observed in the condensed phases, which change from the ordered phase to the isotropic liquid upon irradiation, except for compound **10**, a soft crystal in which a permanent photoalignment highly sensitive to light polarization is produced. The latter is a behavior with potential applications, rather unusual in low-molecular-weight compounds.

Introduction

Liquid crystals are versatile materials for applications.[1] The incorporation of liquid crystals in photoresponsive devices (for optical data storage, photomechanics, or nonlinear optics) is one of the main applications, and several recent reviews on this topic can be found.[2] In order to display functions, the liquid crystal has to contain entities able to react to luminous stimuli. For example, azobenzenes, stilbenes, spirocompounds, etc., undergo either an isomerization or a photochemical reaction when irradiated with the adequate wavelength. Upon irradiation, the shape of the photoreactive entity changes and, as a consequence, different photoinduced effects can be produced, such as changes in color,[3] changes in the molecular orientation,[2a,b,h] isothermal phase transitions,[4] induction of chirality,[5] birefringence,[6] changes in polarization[7] and in magnetism,[8] photomechanical effects,[9] or light-driven plasmonic switching.[2i] These photoresponsive moieties are included in devices as dopants or as part of polymers and also as part of supramolecular self-assemblies.[2j]

Azobenzene and its derivatives are well-known to undergo reversible trans−cis isomerization,[10] which changes the

*To whom correspondence should be addressed. E-mail: espinet@qi.uva.es (P.E.), j.etxeba@ehu.es (J.E.).

(1) Tschierske, C. *J. Mater. Chem.* **2008**, *18*, 2869.

(2) (a) Ichimura, K. *Chem. Rev.* **2000**, *100*, 1847. (b) Natansohn, A.; Rochon, P. *Chem. Rev.* **2002**, *102*, 4139. (c) Shibaev, V.; Bobrovsky, A.; Boiko, N. *Prog. Polym. Sci.* **2003**, *28*, 729. (d) Lemieux, R. P. *Soft Matter* **2005**, *1*, 348. (e) Mizoshita, N.; Seki, T. *Soft Matter* **2006**, *2*, 157. (f) Sato, H.; Yamagishi, A. *J. Photochem. Photobiol. C* **2007**, *8*, 67. (g) Ikeda, T.; Mamiya, J.; Yu, Y. *Angew. Chem., Int. Ed.* **2007**, *46*, 506. (h) Mataharu, A. S.; Jeeva, S.; Ramanujam, P. S. *Chem. Soc. Rev.* **2007**, *36*, 1868. (i) Hsiao, V. K. S.; Zheng, Y. B.; Juluri, B. K.; Huang, T. J. *Adv. Mater.* **2008**, *20*, 3528. (j) Yagai, S.; Kitamura, A. *Chem. Soc. Rev.* **2008**, *37*, 1520. (k) Tejedor, R. M.; Vera, F.; Oriol, L.; Sierra, T.; Serrano, J. L. *Mol. Cryst. Liq. Cryst.* **2008**, *489*, 105.

(3) (a) Sackmann, E. *J. Am. Chem. Soc.* **1971**, *93*, 7088. (b) Irie, M. *Chem. Rev.* **2000**, *100*, 1683. (c) Lee, H.-Y.; Dói, K.; Harada, H.; Tsutsumi, O.; Kanazawa, A.; Shiono, T.; Ikeda, T. *J. Phys. Chem. B* **2000**, *104*, 7023. (d) Bossi, M.; Murgida, D.; Aramendía, P. F. *J. Phys. Chem. B* **2006**, *110*, 13804.

(4) (a) Ikeda, T.; Horiuchi, S.; Karanjit, D. B.; Kurihara, S.; Tazuke, S. *Macromolecules* **1990**, *23*, 36. (b) Ikeda, T.; Horiuchi, S.; Karanjit, D. B.; Kurihara, S.; Tazuke, S. *Macromolecules* **1990**, *23*, 42. (c) Kurihara, S.; Ikeda, T.; Sasaki, T.; Kim, H.-B.; Tazuke, S. *J. Chem. Soc., Chem. Commun.* **1990**, 1751.

(5) (a) Mitsuoka, T.; Sato, H.; Yoshida, J.; Yamagishi, A.; Einaga, Y. *Chem. Mater.* **2006**, *18*, 3442. (b) Yoshida, J.; Sato, H.; Hoshino, N.; Yamagishi, A. *J. Phys. Chem. B* **2008**, *112*, 9677. (c) Tejedor, R. M.; Oriol, L.; Serrano, J. L.; Sierra., T. *J. Mater. Chem.* **2008**, *18*, 2899.

(6) Okano, K.; Shishido, A.; Ikeda., T. *Adv. Mater.* **2006**, *18*, 523.

(7) Walton, H.; Coles, H. *Ferroelectrics* **1993**, *147*, 223.

(8) Nakatsuji, S. *Chem. Soc. Rev.* **2004**, *33*, 348.

(9) (a) Kondo, M.; Yu, Y.; Ikeda, T. *Angew. Chem., Int. Ed.* **2006**, *45*, 1378. (b) Yagai, S.; Iwashima, T.; Kishikawa, K.; Nakahara, S.; Karatsu, T.; Kitamura, A. *Chem.—Eur. J.* **2006**, *12*, 3984.

(10) (a) Rau, H. In *Photochromism. Molecules and Systems*; Dürr, H. B., Bouas-Laurent, H., Eds.; Elsevier: Amsterdam, The Netherlands, 1990; p 165. (b) Rau, H. Photochemistry of Azobenzenes. In *Photochemistry and Photophysics*; Rabek, J. K., Ed.; CRC Press: Boca Raton, FL, 1990; Vol. II.

Published on Web 09/10/2010

molecular geometry (planar rodlike for the trans isomer to nonplanar bent-shaped for the cis isomer) and the dipolar moment of the molecule.[11] Azobenzene-containing compounds have been incorporated in very different systems to obtain photoresponsive materials. There are still very few examples[2f,5a,5b,12−15] where the material involved in the photoreactivity of azo-containing compounds is a metallomesogen.[16] The photoresponsivity is usually studied on isotropic solutions of these compounds, so the property of being a liquid crystal in condensed phases is irrelevant for the photoresponsivity in these cases.[12,13] In most cases, the azo compound is used as a chiral dopant of a nematic solvent, and the isomerization of the azo group induces a change in the pitch value of the cholesteric phase, not a change of the phase.[2f,5a,5b] Only in two cases has the photoresponsivity been proven and studied in the mesophase of the pure compound;[14,15] it is worth noting that the discotic assemblies formed by the macrocyclic azo complex reported in ref 15 show high light sensitivity only in the lyotropic state.

With these few precedents, we aimed at exploring the photoisomerization of the azobenzene function in metal-containing liquid crystals. Some structural types of orthometalated iminepalladium complexes previously reported by our group[17] were conveniently modified to introduce the azobenzene moiety by replacing one or two acetate bridges for 4-(phenylazo)benzoate by 4-[2′,3′,4′-tris(decyloxyphenylazo)]benzoate.[18] The first kind of carboxylate was chosen to check whether the complex with an azobenzene moiety at the bridging position of the dimer was or was not photoresponsive. The second introduces a bulkier moiety, which might affect more effectively the molecular order when the azo function isomerizes.

Scheme 1. Synthesis of **3**[a]

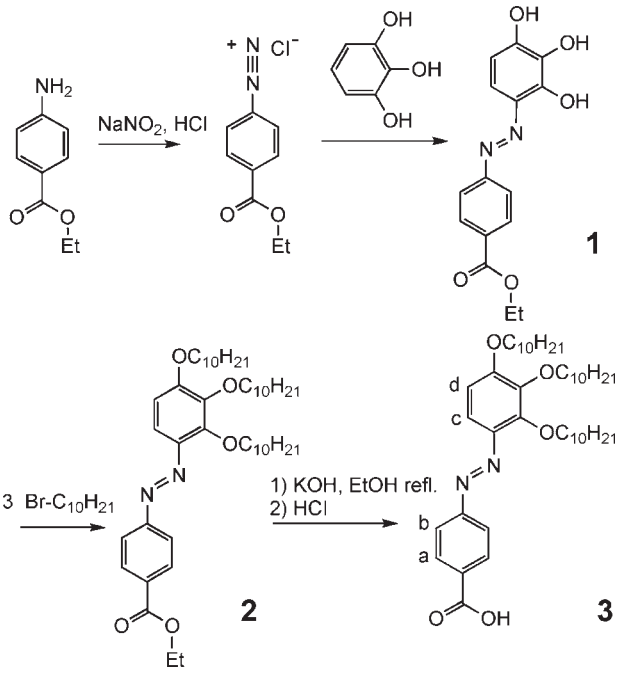

[a]Aryl labels are for the ^{1}H NMR signals.

Results and Discussion

Synthesis and Characterization. The synthesis of 4-[2′,3′,4′-tris(decyloxyphenylazo)]benzoic acid (**3**) was achieved in three steps (Scheme 1). First, an azo coupling between 1,2,3-tris(hydroxybenzene) and the diazonium salt of the corresponding benzoate ester afforded **1**; ^{1}H NMR revealed that the preferred position of coupling was position 4 of the trihydroxybenzene. Then, alkoxylation of the OH groups afforded ester **2**. Finally, treatment of the ester in a refluxing basic medium, followed by acidification, yielded acid **3**.

The dinuclear complexes with one azocarboxylate bridge, **7**−**10**, were obtained from the analogous complexes with orthopalladated imine and chlorothiolato mixed bridges,[17a] by reaction with the silver salt of the azocarboxylic acid (Scheme 2). ^{1}H NMR shows that the relative position of the orthometalated imines is syn, as in the chlorothiolato precursors.

The complexes with two carboxylate bridges, **11** and **12**, were obtained by reaction of the azocarboxylic acid with the corresponding dinuclear hydroxy-bridged complex (Scheme 3).[17b] In this case, ^{1}H NMR shows that the anti isomer is exclusively obtained.

Mesogenic Behavior and Structural Properties. The mesomorphism of the different compounds is shown in Table 1. The transition temperatures and enthalpies correspond to the second cycle for both heating and cooling runs.

Compound **3** displays a monotropic nematic (N) phase upon cooling from the isotropic liquid (I), which is thermally metastable in a range of about 20 °C; upon further cooling, three subsequent crystalline phases are detected. It must be pointed out that in this compound hydrogen bonding between the acidic groups makes the mesogenic entity a dimer bearing six long-chain substituents. This polycatenar dimer might be expected to present a discotic shape,[16h] but,

(11) Kumar, G. S.; Neckers, D. C. *Chem. Re.v* **1989**, *89*, 1915.
(12) (a) Aiello, I.; Ghedhini, M.; La Deda, M.; Pucci, D.; Francescangeli, O. *Eur. J. Inorg. Chem.* **1999**, 1367. (b) Ghedini, M.; Pucci, D.; Crispini, A.; Aiello, I.; Barigelletti, F.; Gessi, A.; Francescangeli, O. *Appl. Organomet. Chem.* **1999**, *13*, 565.
(13) Antharjanam, P. K. S.; Mallia, V. A.; Das, S. *Chem. Mater.* **2002**, *14*, 2687.
(14) Arias, J.; Bardají, M.; Espinet, P.; Folcia, C. L.; Ortega, J.; Etxebarría, J. *Inorg. Chem.* **2009**, *48*, 6205.
(15) Pecinovsky, C. S.; Hatakeyama, E. S.; Gin, D. L. *Adv. Mater.* **2008**, *20*, 174.
(16) A metallomesogen is a metal complex displaying liquid-crystal properties. Reviews on this subject: (a) Giroud-Godquin, A. M.; Maitlis, P. M. *Angew. Chem., Int. Ed. Engl.* **1991**, *30*, 375. (b) Espinet, P.; Esteruelas, M. A.; Oro, L. A.; Serrano, J. L.; Sola, E. *Coord. Chem. Rev.* **1992**, *117*, 215. (c) Hudson, S. A.; Maitlis, P. M. *Chem. Rev.* **1993**, *93*, 681. (d) Serrano, J. L., Ed. *Metallomesogens*; VCH: Weinheim, Germany, 1996. (e) Bruce, D. W. Metal-Containing Liquid Crystals. In *Inorganic Materials*; Bruce, D. W., O'Hare, D., Eds.; Wiley: Chichester, U.K., 1996. (f) Neve, F. *Adv. Mater.* **1996**, *8*, 277. (g) Collison, S. R.; Bruce, D. W. Metallomesogens: Supramolecular Organization of Metal Complexes in Fluid Phases. In *Transition Metal in Supramolecular Chemistry*; Sauvage, J. P., Ed.; Wiley: Chichester, U.K., 1999. (h) Donnio, B.; Bruce, D. W. *Struct. Bonding* (*Berlin*) **1999**, *95*, 193. (i) Donnio, B. *Curr. Opin. Colloid Interface Sci.* **2002**, *7*, 371. (j) Gharbia, M.; Gharbi, A.; Nguyen, H. T.; Malthête, J. *Curr. Opin. Colloid Interface Sci.* **2002**, *7*, 312. (k) Binnemans, K.; Görller-Walrand, C. *Chem. Rev.* **2002**, *102*, 2303. (l) Serrano, J. L.; Sierra, T. *Coord. Chem. Rev.* **2003**, *242*, 73. (m) Lin, I. J. B.; Vasam, C. S. *J. Organomet. Chem.* **2005**, *690*, 3498. (n) Porta, B.; Khamsi, J.; Noveron, J. C. *Curr. Org. Chem.* **2008**, *12*, 1298.
(17) (a) Buey, J.; Diez, G. A.; Espinet, P.; García-Granda, S.; Pérez Carreño, E. *Eur. J. Inorg. Chem.* **1998**, *9*, 1235. (b) Diez, L.; Espinet, P.; Miguel, J. A.; Rodríguez Medina, M. P. *J. Organomet. Chem.* **2005**, *690*, 261.
(18) Complexes bearing palladacycles have been extensively studied as metallomesogens. It is usually easy to modulate their steric and electronic properties. For a general revision, see: Donnio, B.; Bruce, D. W. Liquid crystalline Ortho-Palladated Complexes. In *Palladacycles: Synthesis, Characterization and Applications*; Dupont, J., Pfeffer, M., Eds.; Wiley-VCH: Weinheim, Germany. 2008.

Scheme 2. Synthesis of **7**−**10**[a]

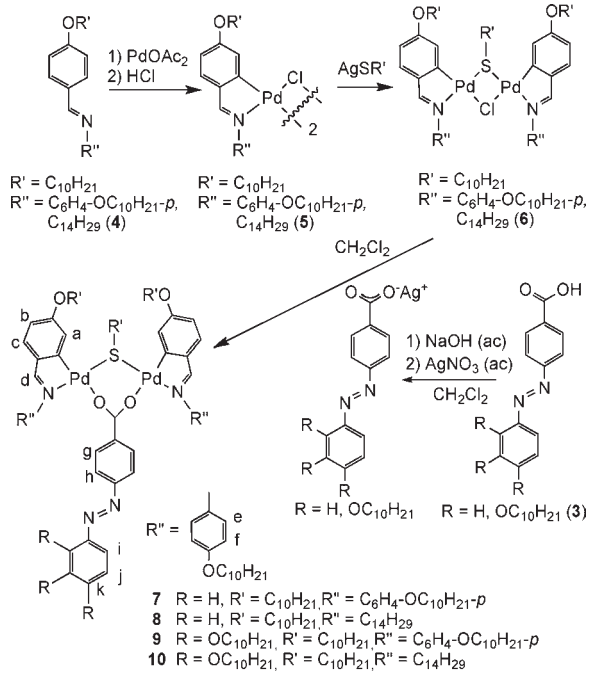

[a]Aryl labels are for the ^{1}H NMR signals.

Scheme 3. Synthesis of **11** and **12**[a]

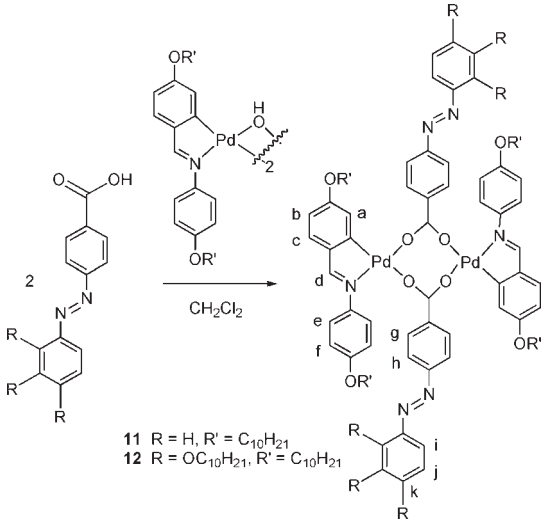

[a]Aryl labels are for ^{1}H NMR signals.

in fact, the nature of the N phase of compound **3** is calamitic (i.e., it is an N phase with positive birefringence). This point was confirmed experimentally: by using a Berek compensator (see the Supporting Information, SI), it was checked that the azobenzene group lies along the rubbing direction of the cell in an oriented sample because this direction determines the slow axis of the optical indicatrix; moreover, this axis coincides with the optic axis of the material, which could be established by measuring the birefringence of the sample as a function of the incidence angle as the sample was rotated along the rubbing direction. The same conclusion was drawn for all of the mesophases studied in the present work and, therefore, the existence of discotic-shaped molecules in the mesophases could be discarded. This conclusion is also supported by the good alignment (see the textures below) obtained in all of the mesophases, which is a typical behavior of calamitic liquid crystals and is hardly observed in the discotic case.

Table 1. Thermal and Thermodynamic Parameters of Compounds **3** and **7**−**12** (Second Heating)[a]

compound	transition	T (°C)	ΔH (kJ·mol^{-1})
3	C → C′	46.4	14.3
	C′ → C″	68.2	3.3
	C″ → C‴	83.4	27.1
	C‴ → I	98.1	−3.5
	(I → N)	(100.0)	(−0.4)
7	C → C′	94.6	−12.3
	C′ → SmA	127.6	13.2
	SmA → N	144.2	0.2
	N → I	155.7	1.3
8	C → I	101.2	56.1
	(I → SmA)	(75.8)	(−1.7)
9	N → I	87.9	0.6
10	C → C′	56.9	12.3
	C′ → C″	64.0	−8.3
	C″ → I	68.5	41.3
	(I → X)	(41.6)	(−0.7)
	(X → C)	(25.5)	(−33.5)
11	C → I	159.2	39.5
	(I → C′)	(147.1)	(−17.1)
	(C′ → C)	(135.6)	(−9.8)
12	C → C′	94.1	2.1
	C′ → I	103.2	63.0

[a]C, C′, C″, C‴ = crystalline phases, N = nematic, SmA = smectic A, I = isotropic liquid, and X = unidentified metastable mesophase. Monotropic transitions are in parentheses.

Compound **7** shows N−SmA mesomorphism, which was determined by texture observations. In compound **8**, only a monotropic SmA phase is observed upon cooling. Compound **9** displays an N phase that gets frozen upon cooling. In the latter compound, the thermogram of the first heating run reveals that two phase transitions are produced (solid−solid and solid−mesophase) before the clearing point, but the solid phase is not recovered upon cooling or in the subsequent heating cycle.

Compound **10** presents a phase sequence with a complicated dynamics, showing kinetic effects involving several metastable phases. Upon heating, DSC data reveal three transitions, including a cold crystallization (see the SI). Upon cooling from the isotropic phase, there is an unidentified phase X, which probably is a mesophase because the transition has a small enthalpy. However, this phase is metastable and could not be studied. X-ray diffraction experiments carried out below the isotropic phase upon cooling actually indicated a crystalline phase. At small angles, a sharp peak and several harmonics were observed (Figure 1a), which might suggest a lamellar structure, and at wide angles, a set of well-defined peaks superimposed to a diffuse halo appeared, indicating that the phase (named C″ in Table 1) is, in fact, a "soft" crystal. The whole X-ray diagram could be indexed (Figure 1a−c). Under the proposed indexation scheme, the corresponding unit cell is monoclinic, with lattice parameters $a = 32.0$ Å, $b = 5.3$ Å, $c = 30.3$ Å, and $\beta = 87.6°$, with b being the monoclinic axis. Essentially the same indexation results at two different temperatures (30 and 40 °C). The identification of this phase as C″ was made by comparing the diffraction patterns obtained upon heating the material from room temperature. In this regard, it must be pointed out that two

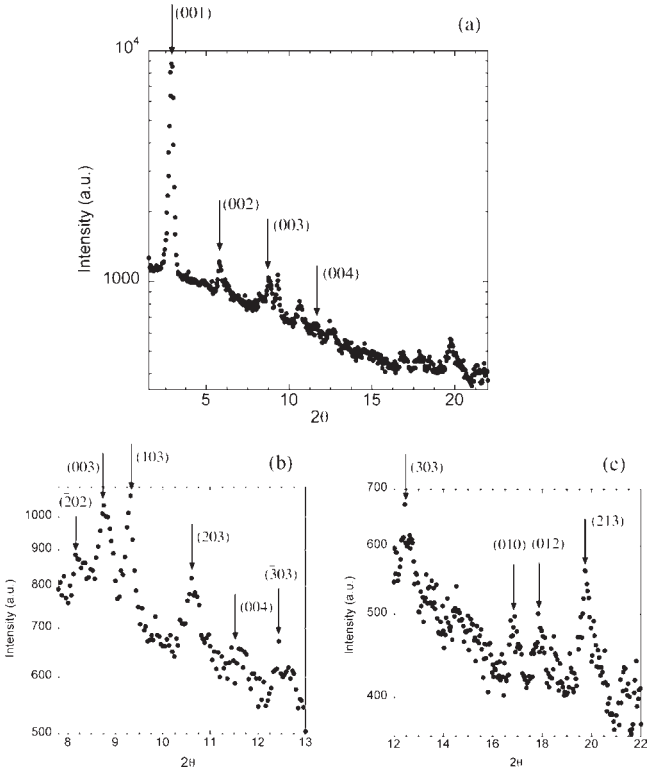

Figure 1. X-ray diffraction pattern of compound **10** as a function of 2θ and the Miller indices: (a) whole diffraction pattern at 30 °C with the (00*l*) reflections indexed; (b and c) detailed wide-angle regions.

additional different patterns, which should correspond to C and C′, were observed at lower temperatures.

Optimization of the molecular structure, using an algorithm based on the CHARMM parametrization,[19] indicates that the molecule has roughly the shape of a rectangular parallelepiped with well-defined sides of about 32 × 15 × 5 Å. The *c* parameter is compatible with the longest molecular distance, which could explain the lamellar-like diffraction pattern observed at small angles because, along the *c* direction, cores would be segregated from tails, giving rise to highly defined X-ray (00*l*) diffraction peaks. On the other hand, the intermediate and small molecular sizes are compatible with two molecules of **10** per unit cell, which would imply a density of 1.26 g·cm^{-3}. This result is in excellent agreement with the measured density of the material (1.27 g·cm^{-3}) and supports the validity of the proposed indexation scheme.

Single crystals were obtained for compound **11** from CH_2Cl_2/petroleum ether. Figure 2 shows the molecular structure determined by X-ray diffraction (see the SI for complete information). The molecular structure is book-shaped, with the two Pd coordination planes making an angle of 26° and the carboxylates in the hinge of the book, as found in related complexes.[17b,20] It is remarkable that

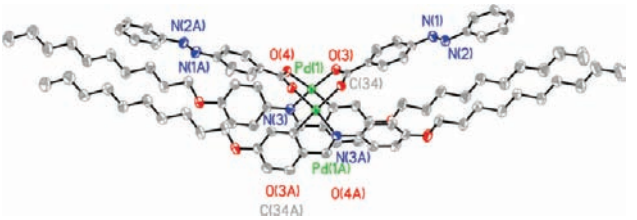

Figure 2. ORTEP diagram for the molecular structure of compound **11**.

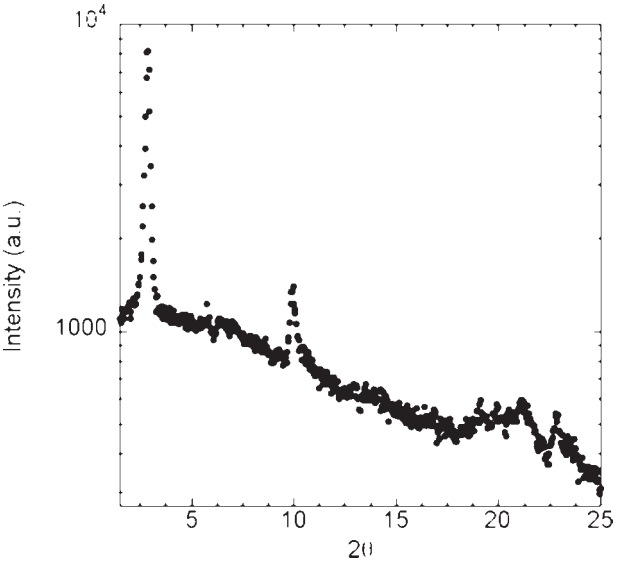

Figure 3. X-ray diffraction pattern vs 2θ of compound **12** at 70 °C.

the palladium coordination planes are almost parallel, making the molecule markedly rodlike. The Pd−Pd distance of 2.92 Å, shorter than twice the van der Waals radius of palladium (3.26 Å) but larger than twice its covalent radius (2.62 Å),[21] is usually considered nonbonding.[20] Upon cooling from the isotropic liquid, compound **11** shows a very viscous monotropic phase, named C′ in Table 1, which could not be aligned. It presents a mosaic texture typical of very ordered smectic phases (B, E, G, H, J, or K). The high enthalpy of the isotropic liquid−C′ phase transition reveals a high molecular order as well.

Finally, compound **12** presents a "soft" crystal phase below the clearing point (named C′ in Table 1). This point was confirmed by X-ray diffraction measurements in the phase (Figure 3). Similar to compound **10**, the material shows a strong peak at small angles that points to a lamellar structure, but at wide angles, several peaks appear over a weak diffuse halo, suggesting a crystalline structure, which is supported by the high melting enthalpy.

Photoisomerization in Solution. UV−Vis Spectra. The new compounds were first tested for their behavior in solution under irradiation by simply recording their electronic spectra before and after their solutions had been irradiated with an intensity of 7 mW·cm^{-2} at a wavelength of 365 nm, near the $\pi \rightarrow \pi^*$ transition band of the trans isomer of azobenzene.[10b] Upon irradiation, the trans starting complexes isomerize to the cis form, giving rise to a severe decrease in the absorbance of the $\pi \rightarrow \pi^*$ band and a slight increase in that of the n $\rightarrow \pi^*$ band of the cis isomer at lower frequencies (Figure 4). The values for the maximum

(19) Brooks, B. R.; Bruccoleri, R. E.; Olafson, B. D.; States, D. J.; Swaminathan, S.; Karplus, M. *Comput. J. Chem.* **1983**, *4*, 187.

(20) Angles found in the literature for acetate-bridged orthopalladated imine complexes range from 25° to 51°. For example, see:(a) Pereira, M. T.; Vila, J. M.; Gayoso, E.; Gayoso, M.; Hiller, W.; Strahle, J. *J. Coord. Chem.* **1988**, *18*, 245. (b) Teijido, B.; Fernández, A.; López-Torres, M.; Castro-Juiz, S.; Suárez, A.; Ortigueira, J. M.; Vila, J. M.; Fernández, J. J. *J. Organomet. Chem.* **2000**, *71*, 598. (c) Castro-Juiz, S.; Fernández, A.; López-Torres, M.; Vázquez-García, D.; Suárez, A. J.; Vila, J. M.; Fernández, J. J. *Organometallics* **2009**, *28*, 6657.

(21) Emsley, J. *The Elements*; Oxford University Press: New York, 1998.

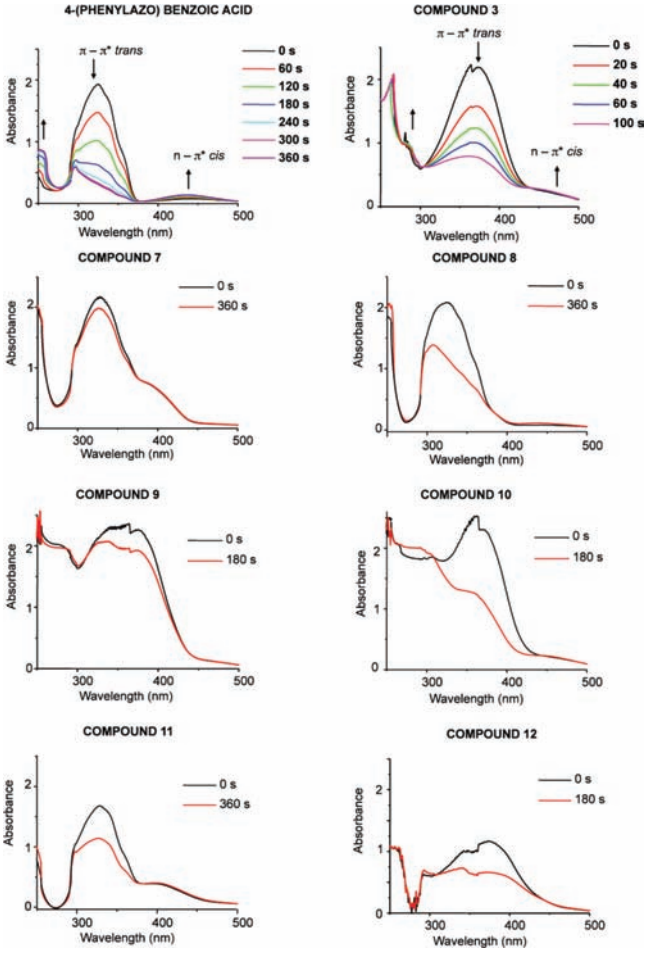

Figure 4. UV−vis spectra in a THF solution before (black line) and after (colored line) irradiation with $\lambda = 365$ nm. The time of exposure is indicated for each compound.

Table 2. Wavelength of Maximum Absorbance and Molar Absorptivity for the Trans Isomer

compound	λ_{max} (nm)	a_{max} ($M^{-1}\cdot cm^{-1}$)
$AzoCO_2H$[a]	326.5	18 500
3	374.0	20 034
7	326.5	59 722
8	325.0	41 086
9	376.0	38 203
10	371.4	35 384
11	327.5	61 098
12	374.0	54 875

[a]4-(Phenylazo)benzoic acid.

absorbance and the correspondent molar absorptivity are listed in Table 2.

The spectra show that all of the complexes are photoresponsive, but to different extent, mainly depending on the electronic distribution over the (phenylazo)benzoato bridge and, apparently, also on how sterically hindered the isomerization is.

The trisubstitution on the phenylazo group causes a bathochromic shift of the $\pi \rightarrow \pi^*$ band, which explains why the complexes with a $3C_{10}AzoCO_2^-$ group are more sensitive to irradiation than those having an azobenzene without chains: It must be noted that the closer the excitation frequency is to the maximum of absorption, the more efficient and faster the trans−cis isomerization process (compare 360 s to reach saturation in 4-(phenylazo)benzoic acid versus 180 s for compound **3**).

Table 3. Maximum Percentage of the Cis Isomer Obtained under Irradiation with $\lambda = 365$ nm and $I = 7$ $mW\cdot cm^{-2}$ (Measured by ^1H NMR Integration)

compound	max cis isomer %	time (min)
3	39	45
7	23	50
8	49	120
9	31	95
10	67	110
11	32	10
12	47	80

On the other hand, the extent of conjugation on the orthometalated imine ligand plays some role (electronic effect and/or steric hindrance) in the trans−cis isomerization because we observe that, independent of the substitution of the azocarboxylato bridge, the complexes bearing the imine with only one phenyl ring (**8** and **10**) respond better to irradiation than those with two phenyl rings in the imine (**7** and **9**). This can be explained by taking into account the two pathways proposed for isomerization of the azo group: an inversion reaction and the N−N rotation.[3c] The presence of the aryl ring in the azobenzene neighborhood is expected to hinder the rotation motion.

The behavior of complexes **11** and **12** is consistent with the proposal that the environment of the azobenzene moiety in the molecule is very important for the photoresponse. In fact, the molecular shapes of **11** and **12**, with the coordination planes of the palladium nearly parallel, make the azocarboxylato groups dangle away from the rigid core and move freely. Thus, their photoresponses are similar and higher than those for the related compounds **7** and **9**.

^1H NMR Spectra. The photoisomerization of the azo group in solution can be sharply observed by ^1H NMR. The experiments were carried out by irradiation of the NMR tubes containing the solutions at 295 K (concentrations ca. 2×10^{-2} M) with the same light as that used in the UV−vis experiment ($\lambda = 365$ nm; $I = 7$ $mW\cdot cm^{-2}$). Before illumination, only the trans isomer was observed. After light exposure, the signals of the two isomers were present, with no signs of decomposition products. All of the NMR peaks were affected by the trans-to-cis isomerization. The most shifted protons were those of the azobenzene moiety because the paramagnetic anisotropic shielding undergone in the cis conformation is stronger. Typically, the shift of the aromatic protons closest to the azo group is about 1 ppm. The chemical shifts of the trans isomers of all of the complexes are given in the Experimental Section. Those of the cis isomers are also given when unambiguous assignment could be made.

In order to check the maximum percentage of the cis isomer that can be obtained under these conditions, the illumination was maintained as far as the resonances of the cis isomer were observed to grow up. The spectra at different irradiation times for **10** are displayed in the SI. A total trans-to-cis-photoinduced transformation was never reached because of competition with the cis-to-trans thermal conversion. Table 3 collects these results. The trend observed is in good accordance with that obtained from the UV−vis measurements.

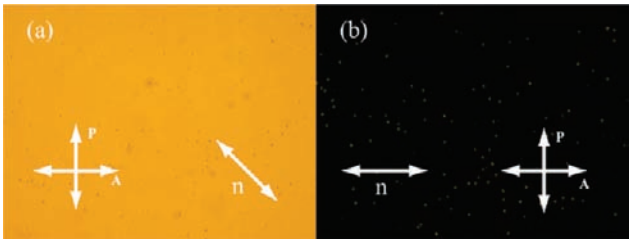

Figure 5. Textures of compound **3** in the N phase at $T = 70$ °C in a planar cell. The good quality of the alignment is clearly observed. Polarizers are at 0° and 90°. The molecular director makes angles of 45° (a) and 0° (b) with respect to the polarizer.

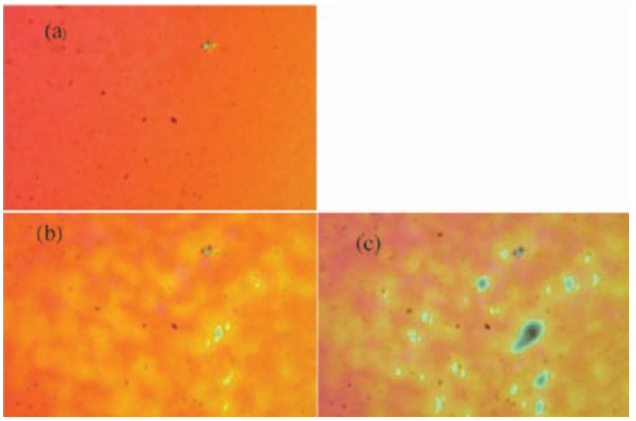

Figure 6. Textures of compound **7** in the N phase at $T = 153$ °C in a planar cell. Polarizers are at 0° and 90°, and the rubbing direction is at 45°. (a) Texture of the virgin sample. The same area is shown after 10 s (b) and 40 s (c) of illumination with the He−Cd laser. The dark areas in part c correspond to the I phase.

Photoisomerization in the Condensed Phases. It is known that the molecular order in the mesophase of azobenzene-containing liquid crystals is disturbed when the calamitic-like trans isomer isomerizes to the bent conformation of the cis isomer.[2a,b,g] Consequently, isotropization of the mesophase can be reached, promoting the trans−cis isomerization by irradiation. In some cases, the trans−cis isomerization only induces a reduction of the birefringence with no change of the mesophase. Below we describe the response of the mesophases of compounds **3** and **7**−**12** to irradiation with a He−Cd laser of wavelength 442 nm and intensity 1 $W \cdot cm^{-2}$, as well as the effects on the birefringence.

Compound 3. The material could be easily aligned in planar cells in the N mesophase (see Figure 5). A birefringence $\Delta n = 0.22$ at 70 °C was obtained. Upon illumination with the laser light, the material underwent an isothermal transition to the isotropic phase. The change was very fast, and the aligned N phase was restored immediately when the illumination was switched off.

Compound 7. The sample showed good planar alignment in both the N and SmA mesophases. A birefringence $\Delta n = 0.23$ was measured in the SmA phase (140 °C), and a slightly lower value was obtained in the N phase. When the material was illuminated for a few seconds in the N phase, a decrease in the birefringence was observed from the original pink color to orange and yellow tones. In contrast to compound **3**, a longer irradiation period was necessary to get black isotropic areas (Figure 6). The change was reversible when the illumination ceased.

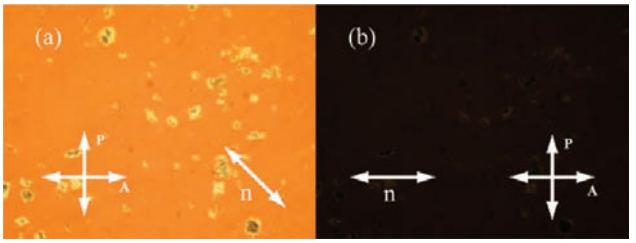

Figure 7. Textures of compound **8** in the SmA phase at $T = 70$ °C in a planar cell. The good quality of the alignment is clearly observed. Polarizers are at 0° and 90°. The molecular director makes angles of 45° (a) and 0° (b) with respect to the polarizer.

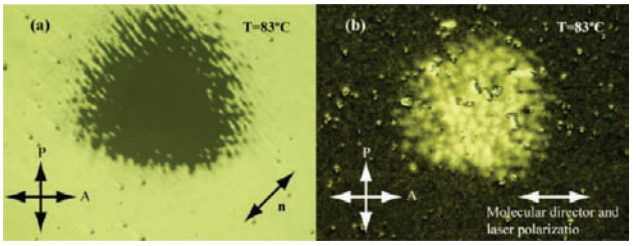

Figure 8. Compound **9** in the N phase. The directions of the polarizer P, analyzer A, and molecular director **n** are indicated. (a) Illumination of the aligned mesophase at 83 °C. The black central area is the I phase. The laser polarization is along the analyzer direction. (b) Illumination of the aligned mesophase at 80 °C. Most of the sample is dark because of the extinction condition. The yellow central area is an N phase that shows no extinction for any rotation angle of the sample. This means that the **n** direction is not well-defined in that region.

The effect is also appreciated in the SmA mesophase, although to a smaller degree. The relatively weak photoresponse can be attributed to the higher difficulty to modify the molecular shape in such a bulky molecule (at least in comparison to compound **3**), leading to just a small percentage of the cis isomer produced (consistent with the solution behavior).

In order to know whether the photoresponse is more effective when illuminated along the director or in a perpendicular direction, the experiment was carried out with crossed polarizers at +45° and −45°, with the optic axis of the material (i.e., the director **n**) being at 0° or 90° and the laser light polarized at 0°. For both phases (SmA and N), the conclusion was the same: the material responded to both polarizations, but the response was more efficient when the polarization was parallel to the director. The result makes sense because the azobenzene group in the trans conformation is dichroic, with maximum absorption for the parallel light.

Compound 8. This material could be aligned in the SmA phase (see Figure 7). The measured birefringence was $\Delta n = 0.20$ at 70 °C. The response to illumination was qualitatively similar to that of both preceding compounds, with an intermediate sensitivity looking at the illumination time required to achieve the isotropic phase. This is also consistent with the behavior observed in solution.

Compound 9. The material has an N phase that could be well aligned, with birefringence $\Delta n = 0.19$ at $T = 83$ °C and $\Delta n = 0.22$ at $T = 65$ °C. In general, the compound responded well to the He−Cd laser light, although the kind of response was temperature-dependent and the effect disappeared soon after the illumination ceased. At 83 °C, the material went rapidly to the I phase (Figure 8a).

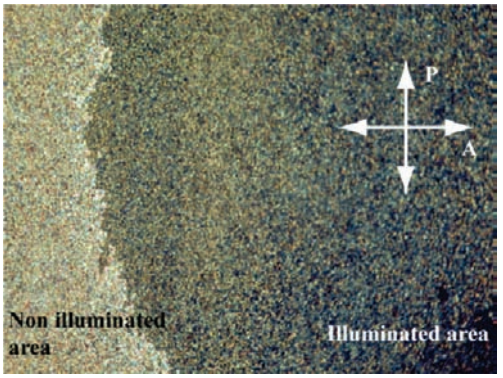

Figure 9. Textures of compound **10** upon cooling from the I phase with the lamp of the microscope switched off (left) or on (right). The illuminated area is darker because of the very small size of the domains, which gives rise to an almost optically isotropic texture.

At 80 °C, the response was different because the laser only modified the alignment of the mesophase, which went to a state where **n** is not very well-defined (bright area in Figure 8b). We think that this can be due to competition between the directions of alignment imposed by the surface treatment and the trend of the illuminated molecules to orient the director perpendicularly to the laser polarization direction. In this material, the response was very sensitive to light polarization. In fact, when the polarization was perpendicular to the director, no effect could be observed. Finally, at 65 °C, the material hardly responded to the light, irrespective of its polarization.

Compound 10. As reported in the Mesogenic Behavior and Structural Properties section, this compound presents an unidentified mesophase X that could not be studied because of its metastability. However, the stable phase C, identified as a "soft" crystal, has a very special behavior with the light. As in the cases above, the material turns out to be marked by the light, but interestingly here the mark remains in the absence of the beam, being permanent at least for 15 h. This persistence has never been reported before for a low-molecular-weight soft crystal (though it is typical for liquid-crystal polymers). In the case of liquid crystals, the relatively low viscosity of the mesophases restores the original alignment in a few seconds after the light is switched off. In the present case, however, the phase is viscous enough to retain the light alignment but soft enough to permit the light to mark the sample. The mark can only be erased by heating to the I phase and cooling down again.

The way the light affects the sample is peculiar and deserves a comment. If the material is cooled down in the dark from the isotropic phase, a small-size domain texture is obtained (Figure 9, left). However, if a moderate light source (e.g., the microscope lamp itself) is on during the cooling process, the domain size is much smaller (Figure 9, right). In fact, in the later conditions, an almost isotropic texture is created (the transmitted intensity is small and independent of the angular position of the sample, i.e., $\Delta n \sim 0$). This suggests that the domain dimensions are on the order of magnitude of the visible wavelength.

It is in this situation where the sample is most sensitive to laser illumination. Figure 10a shows a laser mark (bright area) on this dark texture, where the director of

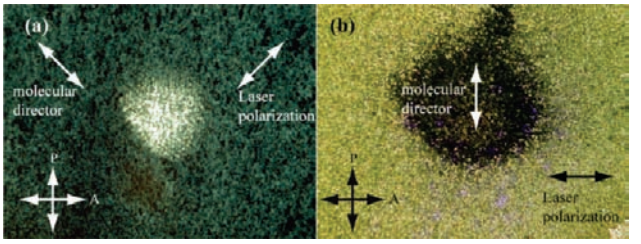

Figure 10. (a) Effect of laser illumination on the optically isotropic texture of compound **10**. A slightly birefringent texture (bright area) is induced, with the director orientation perpendicular to the laser polarization. (b) Mark created on a sample of compound **10** cooled from the I phase under laser illumination. The illuminated area is birefringent and appears dark because the director is parallel to the polarizer P direction.

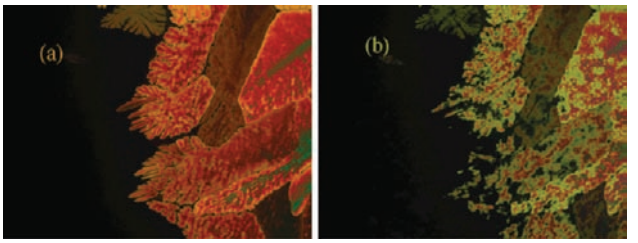

Figure 11. Textures of compound **11** at $T = 146$ °C, in the very vicinity of the clearing point, before (a) and after (b) illumination with the He−Cd laser light. The black area on the left is the I phase.

the induced structure (slow axis of the optical indicatrix) is perpendicular to the laser polarization. The birefringence induced after a few seconds of laser illumination is typically 0.02. In addition, we have checked that, once the mark has been created, a change of the light polarization direction also produces a counterpart in the director orientation, with both being perpendicular to each other in the steady state (the entire reorientation process can last a few minutes).

Upon cooling from the I phase with the laser on, the birefringent mark is directly created, without mediating the optically isotropic texture (Figure 10b). In all cases, the laser produces a permanent photoalignment of the material, where the director direction is controlled by the laser polarization.

Compound 11. The phase below the I phase is metastable and could not be aligned. It is very viscous and probably shows crystalline order. The birefringence has a value of 0.28 at 145 °C. Upon illumination, there was no change to the isotropic liquid (except at very high temperature; see Figure 11), but there is always a reduction in the birefringence. In this case, the high viscosity is another factor that reduces the effect of the light on the phase.

Compound 12. The material showed a soft crystalline phase that could not be aligned. The small domain size prevented the performance of reliable measurements of the birefringence. There was hardly any effect of the laser light on the material texture even close to the clearing point.

Conclusions

Complexes derived from orthopalladated imines bearing one or two azocarboxylato bridges were synthesized, with three of them (**7**−**9**) behaving as liquid crystals, while **10**−**12** are "soft" crystals. Because of the presence of the azobenzene

moiety, these compounds photoisomerize in solution with light of $\lambda = 365$ nm. As deduced from their electronic and ^{1}H NMR spectra, the best responses are achieved when three alkoxy chains are linked to the azo bridge and even better when the orthometalated part of the molecule does not hinder the trans-to-cis motion.

The photoresponse of all compounds has also been studied in their condensed phases. Some parallelism has been found with the behavior in solution, although the particular kind of phase and, especially, its viscosity have turned out to be crucial for the performance of the materials. All of them respond to the light, although to very different degrees, ranging from compound **3** (the free acid, the most sensitive and fast) to compound **12**, which is almost inactive. The case of compound **10**, a soft crystal, is especially interesting, with a moderate but permanent photoresponse and high sensitivity to the light polarization. These properties are unusual and could be used or further elaborated to produce materials for permanent optical memories.

Experimental Section

General Procedures. ^{1}H NMR spectra were recorded in a Bruker AC-300 or ARX-300 MHz spectrometer, in $CDCl_3$. Elemental analyses were done in a Perkin-Elmer 2400 microanalyzer. IR spectra were recorded with a Perkin-Elmer FT 1720X spectrophotometer (4000−400 cm^{-1}) using KBr pellets. The textures of the mesophases were studied with a Leica model DMRB polarizing microscope, equipped with a Mettler FP-82HT hot stage and a Mettler FP-90 temperature controller. Transition temperatures and enthalpies were measured by differential scanning calorimetry (DSC), with a Perkin-Elmer DSC-7, using aluminum crucibles. The apparatus was calibrated with indium (156.6 °C; 28.45 $J \cdot g^{-1}$) as the standard. The electronic spectra were recorded with a Shimadzu UV 1603 UV−vis spectrophotometer from THF solutions. These solutions and those for NMR were irradiated with a UV lamp able to provide light of 254 and 365 nm ($I = 7$ mW·cm^{-2}). Planar samples were prepared in commercially available cells (Linkam) of a nominal thickness of 5 μm. The inner glass surfaces were coated with polyimide and rubbed unidirectionally. Samples were illuminated with polarized laser light, and the textures were simultaneously observed in the polarizing microscope. We employed a He−Cd laser emitting at 442 nm, and the average intensity of irradiation on the samples was about 1 W·cm^{-2}. The birefringence was measured using a Berek compensator. The optical path difference was determined through the rotation angle of a calcite plate cut perpendicular to the polarizing microscope axis.[22] Single-crystal X-ray diffraction was carried out in a Bruker SMART CCD diffractometer. Cell parameters were retrieved using *SMART*[23] software and refined with *SAINT*[24] on all observed reflections. Data reduction was performed with the *SAINT* software and corrected for Lorentz and polarization effects. Absorption corrections were based on multiple scans (program *SADABS*).[25] The structure was solved by direct methods and refined anisotropically on F^2.[26] All non-hydrogen atomic positions were located in difference Fourier maps and refined anisotropically. Powder X-ray diffraction measurements were carried out with a powder diffractometer equipped with a high-temperature attachment. Data were collected in Debye−Scherrer operation mode using Lindemann capillaries of diameter 0.5 mm. A linear position-sensitive detector, with an angular resolution better than 0.01°, was employed to detect the diffracted intensity in the 2θ interval 0.5−35° (θ is the Bragg angle). Monochromatic Cu Kα_1 radiation (1.5406 Å) was used.

Commercial reagents and solvents were used as provided. Literature procedures were used to synthesize the hydroxo-bridged[17b] and thiolatochloro-bridged[17a] precursors. Synthesis of the trisubstituted azocarboxylate was achieved in three steps, as described below, based on the reported synthesis of 4-(4′-*n*-tetradecyloxyphenylazo)benzoic acid,[27] with adequate modifications.

Preparation of 4-[2′,3′,4′-Tris(*n*-decyloxyphenylazo)]benzoic Acid (3). Step 1: Ethyl 4-[(2′,3′,4′-Tris(hydroxyphenylazo)]benzoate (1). A solution of 2.27 g of sodium nitrite (32.04 mmol) in water (15.72 mL) was added dropwise over a suspension of ethyl *p*-aminobenzoate (4.5 g, 26.70 mmol) in a mixture of hydrochloric acid and water (10 and 30 mL, respectively) below 5 °C. The reaction mixture was stirred for 30 min, and then 4.04 g of pyrogallol (32.04 mmol) was added. After stirring for 1 h at ≤5 °C, the cold reaction mixture was poured into a $NaHCO_3$ saturated solution to reach a pH of 6−7. A brown solid appeared that was filtered off and washed with water. This solid was treated with diethyl ether to remove an insoluble fraction. The solution was evaporated, the residue was dissolved in acetone, and the final brown product was precipitated with petroleum ether. Yield: 30%. ^{1}H NMR (300 MHz, acetone-d_6): δ 13.30 (br signal, −OH), 8.15 (d, $J = 8.9$ Hz, 2H), 7.93 (d, $J = 8.9$ Hz, 2H), 7.36 (d, $J = 9.0$ Hz, 1H), 6.67 (d, $J = 9.0$ Hz, 1H), 4.35 (q, $J = 7.3$ Hz, 2H), 3.00 (br signal including −OH), 1.37 (t, 7.3 Hz, 3H). IR (KBr): 3409, 1692, 1604, 1284 cm^{-1}.

Step 2: Ethyl 4-[2′,3′,4′-Tris(*n*-decyloxyphenylazo)]benzoate (2). Over a mixture of **1** (1.18 g, 3.9 mmol), K_2CO_3 (2.7 g, 20 mmol), and KI (0.3 g) in dry acetone (150 mL) under a nitrogen atmosphere was added 1-bromodecane (5.2 g, 23.5 mmol). The reaction was stirred under reflux for 48 h and checked by thin-layer chromatography (silica gel, CH_2Cl_2). The product obtained is a mixture of, at least, the mono-, di-, and trialkoxylated derivatives. The acetone was removed, and the bulk of the reaction was treated with toluene, filtered off, and chromatographed in a silica column, eluting with toluene to collect exclusively the trisubstituted derivative. The product is a red solid after solvent removal. Yield: 29%. Mp: 41.4 °C ($\Delta H = 55.8$ kJ·mol^{-1}). ^{1}H NMR (300 MHz, $CDCl_3$): δ 8.18 (d, $J = 8.7$ Hz, 2H), 7.93 (d, $J = 8.9$ Hz, 2H), 7.52 (d, $J = 9.3$ Hz, 1H), 6.72 (d, $J = 9.3$ Hz, 1H), 4.42 (q, $J = 7.0$ Hz, 2H), 4.25 (t, $J = 6.7$ Hz, 2H), 4.06 (t, $J = 6.7$ Hz, 4H), 1.91−1.79 (m, 6H), 1.57−1.28 (m, 45H), 0.91−0.86 (m, 9H). IR (KBr): 2916, 2851, 1718, 1587, 1472, 1296, 1273 cm^{-1}.

Step 3: Compound 3. Over an ethanolic solution (200 mL) of **2** (0.88 g, 1.2 mmol) was added 0.4 g (8.4 mmol) of solid KOH, and the mixture was refluxed for 5 h. After cooling to room temperature, the reaction was poured into 500 mL of water. Concentrated hydrochloric acid was added to reach an acidic pH. The orange precipitate formed was collected and washed with water, EtOH, and acetone successively. Yield: 85%. ^{1}H NMR (300 MHz, $CDCl_3$): azo group in the trans conformation (see Scheme 1 for labels) δ 8.26 (d, $J = 8.5$ Hz, 2H, Hb), 7.96 (d, $J = 8.5$ Hz, 2H, Ha), 7.54 (d, $J = 9.1$ Hz, 1H, Hc), 6.72 (d, $J = 9.3$ Hz, 1H, Hd), 4.27 (t, $J = 6.4$ Hz, 2H), 4.07 (m, 4H), 1.89−1.80 (m, 6H), 1.51−1.27 (m, 42H), 0.91−0.86 (m, 9H); azo group in the cis conformation δ 7.98 (d, $J = 8.8$ Hz, 2H,

(22) Wahlstrom, E. E. Optical crystallography with particular reference to the use and theory of the polarizing microscope. John Wiley: New York, 1960. See also the comment about the Berek compensator given in the SI.

(23) *SMART software for the CCD Detector System*, version 5.051; Bruker Analytical X-ray Instruments Inc.: Madison, WI, 1998.

(24) *SAINT integration software*, version 6.02; Bruker Analytical X-ray Instruments Inc.: Madison, WI, 1999.

(25) Sheldrick, G. M. *SADABS: A program for absorption correction with the Siemens SMART system*; University of Göttingen; Göttingen, Germany, 1996.

(26) *SHELXTL program system*, version 5.1; Bruker Analytical X-ray Instruments Inc.: Madison, WI, 1998.

(27) Folcia, C. L.; Alonso, I.; Ortega, J.; Etxebarría, J.; Pintre, I.; Ros, M. B. *Chem. Mater.* **2006**, *18*, 4617.

Hb), 6.94 (d, J = 8.7 Hz, 2H, Ha), 6.45 (d, J = 8.8 Hz, 1H, Hc), 6.31 (d, J = 8.8 Hz, 1H, Hd), 4.03 (t, J = 6.4 Hz, 2H), 3.89 (t, J = 6.4 Hz, 2H), 3.78 (t, J = 6.4 Hz, 2H), 1.89−1.80 (m, 6H), 1.51−1.27 (m, 42H), 0.91−0.86 (m, 9H). IR (KBr): 2921, 2851, 2664, 2548, 1692, 1460, 1585, 1286 cm^{-1}. Elem anal. Found (exptl): C, 74.00 (74.31); H, 10.05 (10.15); N, 4.11 (4.03).

Preparation of [Pd(μ-$SC_{10}H_{21}$)(μ-Cl)(L^2)$_2$]. This compound is the precursor of compounds **8** and **10**. Nevertheless, its synthesis is very similar to that reported for other orthopalladated complexes with mixed bridges;[17a] this is the first that is derived from an imine with only one aromatic ring, and thus its characterization as well as that of its precursors is reported here.

1. HL^2, $H_{21}C_{10}OC_6H_4CH{=}NC_{14}H_{29}$ (4). The synthesis was carried out as previously reported.[28] A yellow solid was obtained in 75% yield. Mp: 33.2 °C (ΔH = 62.4 kJ·mol^{-1}). ^{1}H NMR (300 MHz, $CDCl_3$): δ 8.19 (s, 1H), 7.66 (d, J = 8.7 Hz, 2H), 6.91 (d, J = 8.7 Hz, 2H), 3.99 (t, J = 6.6 Hz, 2H), 3.57 (t, J = 6.8 Hz, 2H), 1.83−1.26 (m, 40H), 0.91−0.87 (m, 6H). IR (KBr): 2938, 1634, 1607, 1509, 1470, 1244 cm^{-1}. Elem anal. Found (exptl): C, 81.24 (81.34); H, 11.97 (12.11); N, 3.18 (3.06).

2. [Pd(μ-Cl)L^2]$_2$ (5). Over a hot solution (80 °C) of palladium acetate (0.15 mg, 0.22 mmol) in 30 mL of toluene was added the imine ligand HL^2 (0.3 g, 0.66 mmol). After 2 h of heating, the reaction was slowly cooled down to room temperature. The dinuclear acetate-bridged complex was not isolated. A methanolic solution of hydrochloric acid (0.5 mmol) was added to the bulk of the reaction and stirred for 15 min. The mixture of solvents was removed, and the residue was chromatographed in a silica gel column with CH_2Cl_2 as the eluent. A yellowish solid was obtained after concentration and precipitation with petroleum ether. Yield: 57%. ^{1}H NMR (300 MHz, $CDCl_3$): δ 7.66 (s, 2H), 7.10 (d, J = 8.4 Hz, 2H), 6.90 (d, J = 2.4 Hz, 2H), 6.54 (dd, J = 2.6 and 8.5 Hz, 2H), 3.97 (t, J = 6.4 Hz, 4H), 3.56−3.52 (m, 4H), 1.83−1.76 (m, 8H), 1.56−1.25 (m, 72H), 0.90−0.86 (m, 12H). IR (KBr): 2920, 2849, 1618, 1580, 1467, 1265, 1228 cm^{-1}. Elem anal. Found (exptl): C, 61.81 (62.20); H, 8.95 (9.09); N, 2.36 (2.34). Thermal behavior: C, 103.1 °C (23.7 kJ·mol^{-1}); S_A, 121.9 °C (6.6 kJ·mol^{-1}) I.

3. [Pd(μ-$SC_{10}H_{21}$)(μ-Cl)(L^2)$_2$] (6). This compound was obtained by the method reported in the literature.[17a] A yellowish solid was obtained in 90% yield. ^{1}H NMR (300 MHz, $CDCl_3$): δ 7.79 (s, 2H), 7.31 (d, J = 2.4 Hz, 2H), 7.16 (d, J = 8.3 Hz, 2H), 6.53 (dd, J = 2.4 and 8.3 Hz, 2H), 4.01 (t, J = 6.4 Hz, 4H), 3.56 (br signal, 4H), 2.92 (t, J = 7.2 Hz, 2H), 2.05−1.22 (m, 96H), 0.91−0.87 (m, 15H). IR (KBr): 2921, 2851, 1617, 1580, 1551, 1467, 1265, 1230, 1210 cm^{-1}. Elem anal. Found (exptl): C, 64.69 (64.77); H, 9.53 (9.74); N, 2.15 (2.10). Thermal behavior: C, 26.8 °C (11.8 kJ·mol^{-1}); S_A, 68.1 °C (6.9 kJ·mol^{-1}) I.

Preparation of [Pd_2(μ-$SC_{10}H_{21}$)(μ-O_2CAzo)($L^{1,2}$)$_2$] (7 and 8) and [Pd_2(μ-$SC_{10}H_{21}$)(μ-O_2CAzo3C_{10})($L^{1,2}$)$_2$] (9 and 10). Over a solution of the corresponding acid [4-(phenylazo)benzoic acid (50 mg, 0.15 mmol) or **3** (104 mg, 0.15 mmol)] in CH_2Cl_2 (25 mL) was added 0.3 mL of a 0.5 M solution of NaOH, and the resulting solution was stirred for a few minutes. Then, $AgNO_3$ was added (25 mg, 0.15 mmol) and vigorously stirred for 0.5 h. The palladium complex [Pd(μ-$SC_{10}H_{21}$)(μ-Cl)($L^{1,2}$)$_2$] (0.15 mmol) was dissolved in 25 mL of CH_2Cl_2 and added to the silver salt solution. The reaction was protected from the light and stirred for 4 h. Anhydrous $MgSO_4$ was added to dry the mixture, which was filtered off through a kiesel gel pad. After evaporation of the solvent, the residue was washed with water and then triturated with EtOH. An orange solid was obtained, filtered off, and washed with EtOH and acetone successively. Yield: 85−80%.

Compound 7. ^{1}H NMR (300 MHz, $CDCl_3$; see Scheme 2 for labels): δ 7.92 (dd, J = 2 and 8.2 Hz, 2H, Hi), 7.83 (s, 2H, Hd), 7.67 (d, J = 8.4 Hz, 2H, Hg), 7.55 (d, J = 2.2 Hz, 2H, Ha), 7.53−7.45 (m, 5H, Hh, Hj, Hk), 7.17 (d, J = 8.8 Hz, 4H, He), 7.16 (d, J = 8.8 Hz, 2H, Hc), 6.67 (d, J = 8.8 Hz, 4H, Hf), 6.45 (dd, J = 2.2 and 8.3 Hz, 2H, Hb), 4.1−3.95 (m, 4H), 3.55−3.65 (m, 4H), 2.51 (t, J = 7.4 Hz, 2H), 1.89−1.77 (m, 10H), 1.55−1.10 (m, 70 H), 0.92−0.81 (m, 15H). IR (KBr): 2923, 2853, 1609, 1583, 1546, 1505, 1466, 1390, 1249, 1200 cm^{-1}. Elem anal. Found (exptl): C, 66.87 (66.94); H, 7.94 (8.21); N, 3.45 (3.51).

Compound 8. ^{1}H NMR (300 MHz, $CDCl_3$): azo group in the trans conformation (see Scheme 2 for labels) δ 8.20 (d, J = 8.8 Hz, 2H, Hg), 7.97−7.91 (m, 4H, Hi, Hh), 7.85 (s, 2H, Hd), 7.57−7.49 (m, 3H, Hj, Hk), 7.45 (d, J = 2.6 Hz, 2H, Ha), 7.13 (d, J = 8.4 Hz, 2H, Hc), 6.48 (dd, J = 2.8 and 8.4 Hz, 2H, Hb), 4.08−3.97 (m, 4H), 3.79−3.70 (m, 2H), 3.55−3.47 (m, 2H), 2.46 (t, J = 7.5 Hz, 2H), 1.89−1.77 (m, 10H), 1.55−1.10 (m, 86 H), 0.92−0.81 (m, 15H); azo group in the cis conformation δ 7.97−7.81 (overlapped signal, 2H, Hg), 7.81 (s, 2H, Hd), 7.42 (d, J = 2.4 Hz, 2H, Ha), 7.27−7.14 (m, 3H, Hj, Hk), 7.11 (d, J = 8.3 Hz, 2H, Hc), 6.90−6.85 (m, 2H, Hh), 6.83 (d, J = 8.7 Hz, 2H, Hi), 6.46 (dd, J = 2.6 and 8.2 Hz, 2H, Hb), 4.08−3.97 (m, 4H), 3.69−355 (m, 2H), 3.55−3.38 (m, 2H), 2.39 (t, J = 7.6 Hz, 2H), 1.89−1.77 (m, 10H), 1.55−1.10 (m, 86 H), 0.92−0.81 (m, 15H). IR (KBr): 2922, 2852, 1618, 1586, 1551, 1466, 1390, 1228 cm^{-1}. Elem anal. Found (exptl): C, 66.88 (66.95); H, 9.09 (9.12); N, 3.89 (3.67).

Compound 9. ^{1}H NMR (300 MHz, $CDCl_3$; see Scheme 2 for labels): δ 7.94 (s, 2H, Hd), 7.63 (d, J = 8.6 Hz, 2H, Hg), 7.58 (d, J = 2.3 Hz, 2H, Ha), 7.47 (d, J = 8.6 Hz, 2H, Hc), 7.46 (d, J = 9.1 Hz, 1H, Hi), 7.25−7.21 (m, 6H, He, Hh), 6.71 (d, J = 8.8 Hz, 4H, Hf), 6.69 (d, J = 9.2 Hz, 1H, Hj), 6.51 (dd, J = 2.1 and 8.3 Hz, 2H, Hb), 4.25 (t, J = 6.6 Hz, 2H), 4.10−4.04 (m, 8H), 3.76−3.70 (br signal, 4H), 2.51 (t, J = 7.4 Hz, 2H), 1.89−1.20 (m, 128H), 0.94−0.83 (m, 24H). IR (KBr): 2924, 2853, 1582, 1548, 1507, 1467, 1388, 1288, 1252, 1198 cm^{-1}. Elem anal. Found (exptl): C, 68.97 (69.19); H, 9.15 (9.27); N, 2.79 (2.71).

Compound 10. ^{1}H NMR (300 MHz, $CDCl_3$): azo group in the trans conformation (see Scheme 2 for labels) δ 8.17 (d, J = 8.8 Hz, 2H, Hg), 7.89 (d, J = 8.5 Hz, 2H, Hh), 7.85 (s, 2H, Hd), 7.51 (d, J = 9.1 Hz, 1H, Hi), 7.45 (d, J = 2.7 Hz, 2H, Ha), 7.13 (d, J = 8.4 Hz, 2H, Hc), 6.71 (d, J = 9.2 Hz, 1H, Hj), 6.48 (dd, J = 2.2 and 8.4 Hz, 2H, Hb), 4.25 (t, J = 6.6 Hz, 2H), 4.09−4.00 (m, 8H), 3.77−3.73 (m, 2H), 3.51−3.47 (m, 2H), 2.45 (t, J = 7.4 Hz, 2H), 1.86−1.17 (m, 144H), 0.92−0.81 (m, 24H); azo group in the cis conformation δ 7.89 (d, J = 8.5 Hz, 2H, Hg), 7.81 (s, 2H, Hd), 7.42 (d, J = 2.3 Hz, 2H, Ha), 7.10 (d, J = 8.4 Hz, 2H, Hc), 6.88 (d, J = 8.6 Hz, 2H, Hh), 6.46 (dd, J = 2.2 and 8.3 Hz, 2H, Hb), 6.37 (d, J = 8.9 Hz, 1H, Hi), 6.17, (d, J = 8.8 Hz, 1H, Hj), 4.25 (t, J = 6.6 Hz, 2H), 4.09−4.00 (m, 8H), 3.75−3.55 (m, 4H), 2.40 (t, J = 7.4 Hz, 2H), 1.86−1.17 (m, 144H), 0.92−0.81 (m, 24H). IR (KBr): 2922, 2852, 1586, 1553, 1466, 1392, 1289 cm^{-1}. Elem anal. Found (exptl): C, 68.61 (68.69); H, 9.92 (9.98); N, 2.85 (2.79).

Preparation of [Pd(μ-O_2CAzo)L^1]$_2$(11) and [Pd(μ-O_2CAzo-3C_{10})L^1]$_2$ (12). Over a suspension of [Pd(μ-OH)L^1]$_2$ (0.1 mmol) and $MgSO_4$ in dry CH_2Cl_2 was added 0.2 mmol of the corresponding acid [4-(phenylazo)benzoic acid or compound **3**]. The mixture was stirred for 6 h and filtered off through a pad of kiesel gel. After solvent removal, the solid residue was recrystallized from CH_2Cl_2/EtOH to obtain an orange solid. Yield: 78−80%.

Compound 11. ^{1}H NMR (300 MHz, $CDCl_3$; see Scheme 3 for labels): δ 8.25 (d, J = 8.7 Hz, 4H, Hh), 7.94 (dd, J = 2.2 and 8.1 Hz, 4H, Hi), 7.88 (d, J = 8.5 Hz, 4H, Hg), 7.58 (s, 2H, Hd), 7.53−7.50 (m, 6H, Hj, Hk), 7.19 (d, J = 8.3 Hz, 2H, Hc), 6.73 (d, J = 8.9 Hz, 4H, He), 6.55 (dd, J = 2.3 and 8.0 Hz, 2H, Hb), 6.47 (d, J = 8.8 Hz, 4H, Hf), 6.01 (d, J = 2.2 Hz, 2H, Ha), 3.77 (m, 2H), 3.65 (m, 2H), 3.40 (m, 2H), 3.00 (m, 2H), 1.88−1.07 (m, 64H), 0.91−0.84 (m, 12H). IR (KBr): 2922, 2852, 1606, 1578,

(28) Baena, M. J.; Espinet, P.; Ros, M. B.; Serrano, J. L. *J. Mater. Chem.* **1996**, *6*, 1291.

1561, 1507, 1466, 1384, 1256, 1230, 1199 cm^{-1}. Found (exptl): C, 66.79 (67.02); H, 6.95 (7.21); N 4.88 (5.10).

Compound 12. ^{1}H NMR (300 MHz, $CDCl_3$; see Scheme 3 for labels): δ 8.21 (d, J = 8.4 Hz, 4H, Hh), 7.84 (d, J = 8.4 Hz, 4H, Hg), 7.58 (s, 2H, Hd), 7.51 (d, J = 9.2 Hz, 2H, Hi), 7.18 (d, J = 8.4 Hz, 2H, Hc), 6.74 (d, J = 8.9 Hz, 4H, He), 6.69 (d, J = 9.7 Hz, 2H, Hj), 6.54 (dd, J = 2.1 and 8.4 Hz, 2H, Hb), 6.47 (d, J = 8.9 Hz, 4H, Hf), 6.01 (d, J = 2.2 Hz, 2H, Ha), 4.24 (t, J = 6.6 Hz, 4H), 4.08−4.02 (m, 8H), 3.77 (m, 2H), 3.65 (m, 2H), 3.40 (m, 2H), 3.00 (m, 2H), 1.88−1.07 (m, 160H), 0.91−0.84 (m, 30H). IR (KBr): 2922, 2854, 1604, 1579, 1560, 1466, 1385, 1289, 1253, 1228, 1198 cm^{-1}. Found (exptl): C, 70.51 (70.59); H, 8.92 (9.26); N, 3.12 (3.25).

Acknowledgment. We gratefully acknowledge financial support by the DGI (Project CTQ2008-03954/BQU and INTECAT Consolider Ingenio-2010 CSD2006-0003), the Junta de Castilla y León (Projects VA012A08 and GR169), the Basque Government (GIC10/45), and the MICIIN (Project MAT2009-14636-C03-03).

Supporting Information Available: DSC thermograms for compounds **2**−**12**, microphotographs for Figures 5−11 depicted at a higher size, ^{1}H NMR spectra for compound **10** after different irradiation times, comment on the Berek compensator, X-ray diffraction data for compound **11**, and X-ray crystallographic data for compound **11** in CIF format. This material is available free of charge via the Internet at http://pubs.acs.org.